

Article

Dependence of Catalyst Surface in Photocatalytic Degradation of Phenyl Urea Herbicides

Sutaporn Meephon¹, Somchintana Puttamat², and Varong Pavarajarn^{1,3,*}

¹ Center of Excellence in Particle Technology, Department of Chemical Engineering, Faculty of Engineering, Chulalongkorn University, Bangkok, Thailand

² Department of Chemistry, Faculty of Science, Thammasat University, Pathumthani, Thailand

³ Research Program in Hazardous Substance Management in Agricultural Industry, Center of Excellence on Hazardous Substance Management (HSM), Bangkok, Thailand

*E-mail: Varong.p@chula.ac.th (Corresponding author)

Abstract. Photocatalytic degradations of various contaminants using in-house synthesized catalysts have been generally reported, but the degradation intermediates formed are normally inconsistent. This issue is particularly important for the degradation of toxic compounds which may form intermediates with increased toxicity. This work resolves this issue by systematically investigating adsorption and photocatalytic degradation of diuron, linuron, and 3,4-dichloroaniline (DCA) on two forms of zinc oxide (ZnO), i.e., conventional particles with zinc- and oxygen-terminated polar surfaces, and nanorods with mixed-terminated non-polar surfaces. Experimental results indicate that both rate of degradation and degradation pathway depend upon the adsorption configuration of the compound undergoing the degradation onto the surface of the catalyst. The adsorption configuration is surface dependent. On polar surfaces, both aliphatic and aromatic sides of diuron and linuron molecules adsorb on the surface, allowing the attack of hydroxyl radicals on both ends. On the other hand, on non-polar surface, only the aliphatic chain adsorbs onto the surface, resulting in the hydroxyl radicals attack only on the aliphatic side. The structure of the catalyst is therefore a crucial factor determining the dominant degradation pathway.

Keywords: Photocatalysis, degradation, pathway, surface dependence.

ENGINEERING JOURNAL Volume 22 Issue 5

Received 29 May 2018

Accepted 9 July 2018

Published 30 September 2018

Online at <http://www.engj.org/>

DOI:10.4186/ej.2018.22.5.57

1. Introduction

Serious water contaminations in many agricultural countries are the results from leaching of residual herbicides [1, 2]. Phenyl urea herbicides, such as diuron [3-(3,4-dichlorophenyl)-1,1-dimethyl urea] and linuron [3-(3,4-dichlorophenyl)-1-methoxy-1-methylurea], are specially problematic because not only they are highly toxic [3], but they are also highly recalcitrant [4]. Many processes have been applied in an attempt to remediate water contaminated with these herbicides [5, 6], but their typically low concentration renders these techniques ineffective.

Heterogeneous photocatalytic degradation is a technique capable of removal of toxic contaminants in water [7, 8]. The process relies on oxidation of the pollutant, which is adsorbed on surface of the photocatalyst, by highly active hydroxyl radicals ($\text{OH}\bullet$). In aqueous solution, the radicals are produced by the reactions between photogenerated holes (h^+) and surrounding water or hydroxyl ions [9]. Although the hydroxyl radicals are strong oxidizer, the degradation of the contaminants usually involves several intermediates. A number of researches have reported the degradation of the same compound using the same kind of catalyst [10-12], but the intermediates detected are usually different. This issue is particularly important and needs to be resolved, especially for the degradation of toxic contaminants, because some intermediates may be more toxic than their parent compounds [13, 14] and benign pathways are desired.

It is a common knowledge that the adsorption is surface dependent, but its subsequent effect on the formation of the degradation intermediates has not been thoroughly investigated. This work provides supports that the variations in the intermediates are the result from the difference in adsorption configuration on the surface of the catalyst. Wurtzite zinc oxide (ZnO) was chosen as the catalyst in this study because it could be synthesized in a manner such that the exposed surfaces could be controlled [15]. Two main sets of ZnO surfaces were considered; (i) zinc-terminated (0001) and oxygen-terminated ($000\bar{1}$) polar surfaces located on top and bottom planes of the hexagonal ZnO crystal, and (ii) mixed-terminated ($10\bar{1}0$) non-polar surface appeared as the side planes of the crystal. Two types of ZnO were used, i.e., conventional ZnO particles, of which the main exposed surfaces, are polar surfaces, and ZnO nanorods, which are consisted mainly of the mixed-terminated surface. Diuron and linuron, as well as 3,4-dichloroaniline (DCA), which shares similar molecular structure as diuron and linuron (see Fig. 1), were studied as the compounds to be degraded.

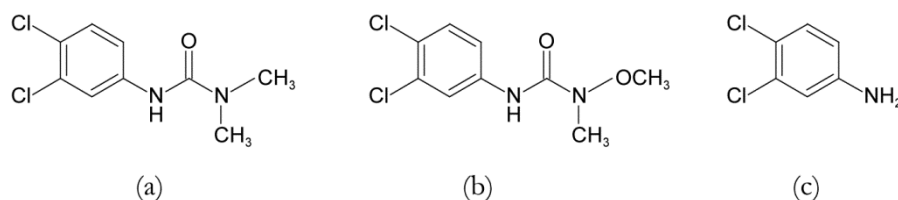


Fig. 1. Molecular structures of diuron (a), linuron (b), and DCA (c).

2. Materials and Methods

2.1. Syntheses of ZnO

Conventional ZnO powder was synthesized via the sol-gel technique. A mixture containing ethanol, diethanolamine, hydrochloric acid, and deionized water in amounts of 5, 1.58, 0.18, and 0.25 mL, respectively, was slowly dropped into a solution of zinc acetate (3.29 g) in 20 mL of deionized water. The mixture was stirred for 2 h and was aged without stirring for 24 h. After being dried at 80°C overnight, the mixture was transformed into a gel. The gel was aged further for 3 days before being calcined at 500°C for 2 h to obtain ZnO powder.

On the other hand, ZnO nanorods were synthesized via the hydrothermal method. A precursor solution was prepared from 1.1 g of zinc acetate in 4 mL of deionized water and 6 mL of 8 M sodium hydroxide aqueous solution. Then, 2 mL of the precursor solution was mixed with 5 mL of polyethylene glycol and 20 mL of ethanol. The mixture was heated at 140°C for 1 h under autogenous pressure in a

Teflon-lined autoclave. The precipitate was washed with ethanol and deionized water before being dried at 60°C overnight.

2.2. Adsorption Studies

In the studies of adsorption of diuron, linuron and DCA onto two types of ZnO catalyst, aqueous solutions of the adsorbate was prepared with concentrations in the range of 0-25 mg/L. The adsorption was conducted by immersing the catalyst into the solution, of which the temperature was controlled to $25 \pm 2^\circ\text{C}$. The catalyst content was 1 mg/mL of the solution. The system was kept in the dark for 6 h, which was experimentally determined to be sufficient to reach adsorption equilibrium. Then, the equilibrium concentration of the solution was determined by reverse-phase high-performance liquid chromatography (HPLC, Shimadzu Class 10VP) [16].

2.3. Photocatalytic Degradation

The photocatalytic degradation was conducted in a microreactor, in which the mass transfer resistance for the transport of the compound undergoing degradation to the surface of the catalyst could be neglected [16]. Moreover, the residence time for the reaction could be easily controlled, enabling us to determine the sequence of the intermediates formed from the degradation. The microreactor was fabricated in a plate-like manner. A piece of glass that had been coated by 6.8 mg of the catalyst via spin-coating was assembled with another piece of glass into which inlet and outlet streams had been drilled. A Teflon sheet with a 0.8 cm \times 4.8 cm opening was placed between the pieces of glass, forming a channel. The height of the channel was determined by the thickness of the Teflon sheet (250 μm). The microreactor assembly was then mounted in a stainless-steel housing.

A 10 ppm aqueous solution of herbicides was constantly supplied into the microreactor via a syringe pump for 1 h prior to the irradiation to ensure complete adsorption onto the catalyst. Then, the reactor was irradiated with light from a 40-W mercury lamp (Philips F40T12/BL), with an emission spectrum in the wavelength range of 350-410 nm, to initiate the reaction. The power flux at the location of the reactor was found to be 3.18×10^{-6} W/cm², measured by an ILT1700 Research Radiometer (International Light Technologies) with SED005 GaAsP UV detector. The flowrate was controlled to correspond to the desired residence time in the range of 1-15 min. The concentration of the compound undergoing degradation was monitored at the outlet by HPLC. After reaching a steady state, a sample was collected for identification of the intermediates via liquid chromatography equipped with tandem mass spectroscopy (LC-MS/MS, Thermo Finnigan, LCQ Advantage). It should be noted that, according to a preliminary test using inductively coupled plasma optical emission spectroscopy (ICP-OES, PerkinElmer Optima7000DV), less than 0.5% of the catalyst detached from the reactor throughout the whole period of the experiment.

3. Results and Discussion

3.1. Characteristics of the Catalysts

Micrographs shown in Fig. 2 indicate that ZnO synthesized by both techniques are significantly different in particle size and morphology. On one hand, the conventional ZnO particles obtained from the sol-gel technique are micron-sized with low aspect ratio. The hexagonal plane, which is either the (0001) or (000 $\bar{1}$) surface, is clearly visible. On the other hand, the ZnO nanorods synthesized via the hydrothermal method are about 50 nm in diameter and about 300-400 nm in length. The dominating plane is the (10 $\bar{1}$ 0) surface. The specific surface area of the nanorods, as measured by nitrogen adsorption/desorption using a Brunauer-Emmett-Teller (BET) analyzer (Belsorp mini II), is much higher than that of the conventional particles, i.e., 17 m²/g versus 1.4 m²/g. According to X-ray diffraction analyses, both catalysts are ZnO in wurtzite phase without contamination from other crystalline phases. The selected-area electron diffraction (SAED) patterns confirm that both catalysts are indeed single crystals (see insets in Fig. 2). An X-ray photoelectron spectroscopy (XPS, Kratos DLD) revealed that both catalysts contain only zinc and oxygen. The high-resolution XPS scan of O1s indicated three states of oxygen, i.e., oxygen in hydroxyl group, oxygen vacancies, and oxygen in ZnO lattice, locating at the binding energy of 532.2, 531.0, and 530.0 eV, respectively (see Fig. 3). The contents of each state of oxygen in both catalysts are about the same,

indicating similar surface functional groups of these catalysts. The optical bandgaps of both catalysts, calculated from Tauc plots measured by reflective UV/Visible spectroscopy, are the same at 3.1 eV. Hence, the major difference between these catalysts is their exposing surfaces.

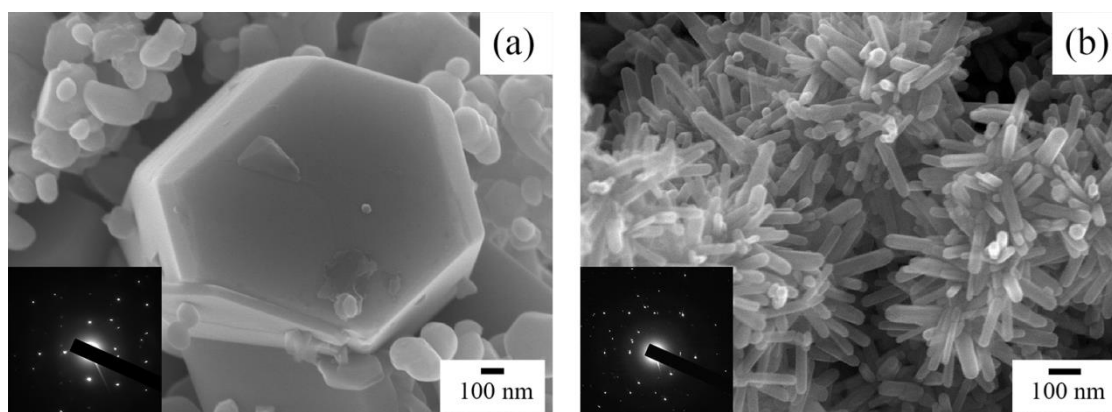


Fig. 2. Scanning electron micrographs and selected-area electron diffraction patterns (shown as inset) of conventional ZnO powder synthesized by sol-gel technique (a) and ZnO nanorods synthesized by hydrothermal method (b).

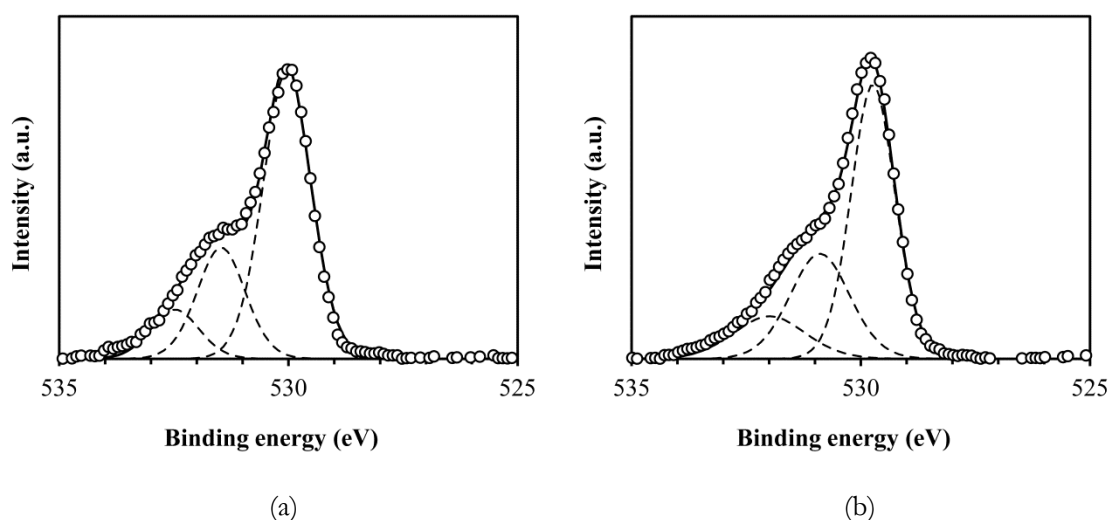


Fig. 3. X-ray photoelectron spectroscopy of conventional ZnO powder synthesized by sol-gel technique (a) and ZnO nanorods synthesized by hydrothermal method (b).

3.2. Adsorption Results

After the adsorption experiments, the obtained results were fitted with various adsorption isotherm models. It was found that the Freundlich isotherm represents the adsorption data well (see Fig. 4). All fitted parameters from the Freundlich model are shown in Table 1. The values of $1/n$ for all cases are less than 1, which indicate that adsorptions of diuron, linuron, and DCA on both types of ZnO catalysts are physical adsorption [17]. This is consistent with the fact that the Langmuir adsorption model, which best describes chemisorption, failed to fit the experimental data. Furthermore, according to Fourier transform infrared spectroscopic analyses of the used catalysts, no signal corresponding to a new bond between the adsorbates and the catalysts was detected.

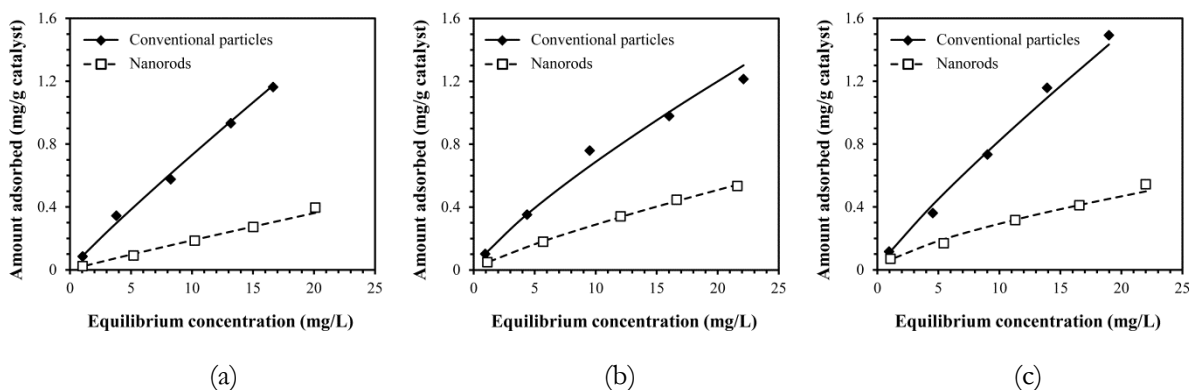


Fig. 4. Experimental data fitted with Freundlich model for adsorption isotherm of diuron (a), linuron (b), and DCA (c) on conventional ZnO particles (solid lines) and ZnO nanorods (dash lines).

Table 1. Fitted parameters for Freundlich adsorption model.

Parameter	On conventional ZnO particles			On ZnO nanorods		
	DCA	Diuron	Linuron	DCA	Diuron	Linuron
K_f	0.110	0.082	0.101	0.049	0.028	0.036
$1/n$	0.868	0.959	0.849	0.772	0.815	0.901
R^2	0.992	0.983	0.998	0.976	0.978	0.999

The fitted parameter relating to adsorption capacity (K_f) for adsorption on the conventional ZnO particles is about twice the value for the nanorods. They clearly show that greater amounts of all investigated adsorbates were adsorbed on the conventional ZnO particles than on the ZnO nanorods, even though the surface area of the former is one order of magnitude lower than the latter. Zinc- and oxygen-terminated polar surfaces are composed of only one kind of atom on the surface, while the mixed-terminated surface is formed by alternate arrangement of zinc and oxygen atoms. The non-polar mixed-terminated surface of the nanorods does not possess electrostatic instability and hence is less active in adsorption than the polar surfaces [18, 19].

For diuron and linuron, polar parts of the molecules are attracted to high affinity of polar surfaces of the conventional ZnO particles. Interestingly, the molecules of diuron and linuron are consisted of both negatively and positively charged parts, which enable them to be adsorbed onto both zinc- and oxygen-terminated surfaces of the conventional ZnO particles. The highly positively charged region is located on hydrogen atoms adjacent to high-electronegativity atom such as nitrogen and oxygen [20, 21]. This part of the molecule is predicted to adsorb onto oxygen-terminated surface and form weak hydrogen bond with oxygen atoms on the surface [22]. The most negatively charged area of diuron and linuron is located at oxygen atom of the carbonyl group, which is expected to adsorb onto zinc-terminated surface. For DCA, hydrogen atoms of its amine group is the most positively charged part of the molecule, while the nitrogen and chlorine atoms are negatively charged [23]. These parts are expected to adsorb onto polar surfaces in the same manner as diuron and linuron.

Among all three adsorbates investigated, the adsorption capacity of DCA is significantly higher than that of diuron and linuron. It is expected to be the result from small molecular size of DCA, which allows more DCA molecules to be accommodated on the surface. Between diuron and linuron, which share very similar molecular structure, K_f of linuron are higher than that of diuron. This is due to additional negatively charged area on aliphatic chain of linuron, i.e., its alkoxy group, which increases opportunity in adsorption [21]. It should be noted that high-electronegativity oxygen atom in the alkoxy group of linuron, which is the expected part of the molecule to adsorb onto ZnO surface, is connected to a methyl group by a rotatable single bond, allowing the linuron molecule to easily adjust its configuration for adsorption. On the other hand, for diuron, reconfiguration of the molecule to let its oxygen atom to adsorb onto the surface is more difficult because the oxygen is bonded by a non-rotatable double bond.

3.3. Photocatalytic Degradation

The photocatalytic oxidation of an organic compound adsorbed on a catalyst can in principle take place via direct oxidation by photogenerated holes or via indirect oxidation by hydroxyl radicals. For the degradation in aqueous solution, the indirect oxidation is more likely to occur because of the plentiful amount of water surrounding the catalyst. More importantly, it has been reported that chemisorption is a prerequisite for direct oxidation while physisorption favors indirect oxidation [24]. Since, the adsorptions of all species investigated are physisorption (see previous section), it is confirmed that the photocatalytic degradations in this work occurs via indirect oxidation.

The photocatalytic degradation results are shown in Fig. 5. It should be noted that the photolysis degradations of all investigated contaminants are negligible in absence of the catalyst even at the longest residence time. For all experiments, masses of the catalysts used are the same. Therefore, according to the findings from the adsorption studies, the amounts of contaminants adsorbed onto the conventional ZnO particles are much greater than those on the nanorods. However, for diuron and linuron, the degradations on both catalysts are insignificantly different, which implies that the rates of degradation on the mixed-terminated surface of the nanorods are much faster than those on polar surfaces of the conventional ZnO particles. Upon the irradiation of light, both catalysts are expected to generate roughly the same amount of holes because they both have the same energy bandgap. However, the small size of the nanorods facilitates holes transport to the surface of the particles. Furthermore, its large interfacial area increases the chance for the interaction between the holes and the adsorbed water to generate more hydroxyl radicals than that on the conventional ZnO particles. Nevertheless, this is not the only factor affecting the rate of degradation, since it is not applicable for the DCA degradation results.

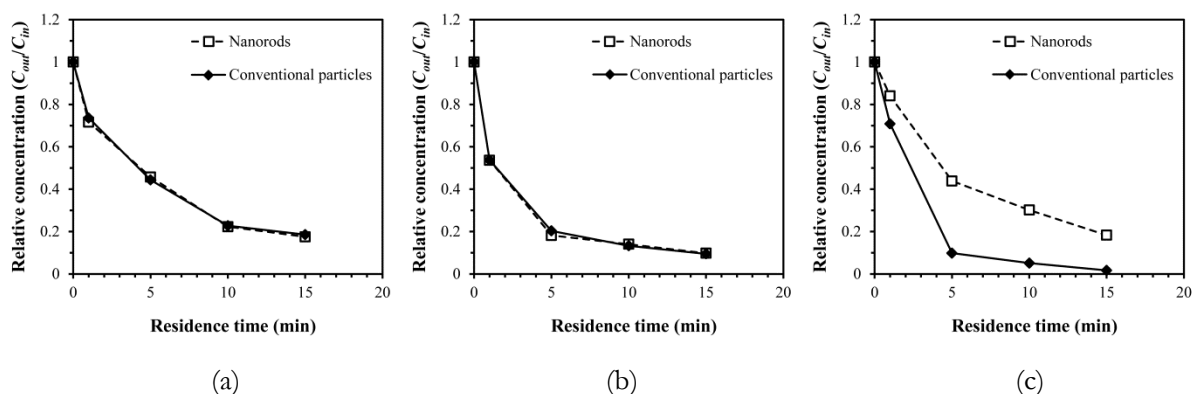


Fig. 5. Photocatalytic degradation results of diuron (a), linuron (b), and DCA (c) on conventional ZnO particles (solid lines) and ZnO nanorods (dash lines).

The major difference between DCA and diuron or linuron is the lack of aliphatic moiety. The attack of hydroxyl radical on DCA molecule occurs on its aromatic ring, while the attack on either diuron or linuron can take place on either aliphatic or aromatic side, depending on the adsorption configurations. Because the aromatic ring is much more stable than the aliphatic part of the molecule, as witnessed from the widely reported observation that ring-opening is the last step of the degradation pathway [25-27], the hydroxyl radical attack on the aromatic side is not as effective toward the degradation as that on the aliphatic side. Hence, amount of DCA adsorbed on the surface is the key factor controlling the degradation rate, which agrees with the experimental observation that the degradation of DCA on the conventional ZnO particles is much faster than that on the ZnO nanorods (see Fig. 5c). The fact that the degradation behaviors of diuron and linuron are not the same as that of DCA also suggests that the adsorption configurations of diuron and linuron onto ZnO surfaces involve their aliphatic moiety. This is consistent with the discussion in the previous section and the report in literature [28].

Comparing between diuron and linuron, the degradation rate of linuron is higher than that of diuron because of the higher reactivity of linuron [29]. The polarization of oxygen atom in the alkoxy group of linuron results in decreased stability of the molecule [30].

3.4. Degradation Intermediates

The outlet stream from the reactor was collected and analyzed by LC-MS/MS to determine the structures of the degradation products. Fig. 6 and 7 report the major intermediates detected at different residence time of diuron and linuron degradations, respectively. The pathways are inferred from the molecular structures of the intermediates. It should be noted that no intermediate was detected from the photolysis of diuron and linuron in absence of a catalyst. In the presence of the catalyst, intermediates were detected in the experiments with residence time of at least 1 min. It is therefore assumed that the intermediates detected at the residence time of 1 min were derived from photocatalytic degradations of the herbicides. It should be mentioned that the concentrations of the detected intermediates could not be measured because of the lack of commercial standard reference compounds. However, all of the intermediates reported in Figs. 6 and 7 were assumed to have concentrations in the same order of magnitude because their corresponding chromatographic peak heights were similar. All paths shown are therefore major degradation pathways. For DCA, unfortunately, the LC-MS/MS analysis failed to reliably identify the intermediates because of small molecular size of DCA and its degradation intermediates.

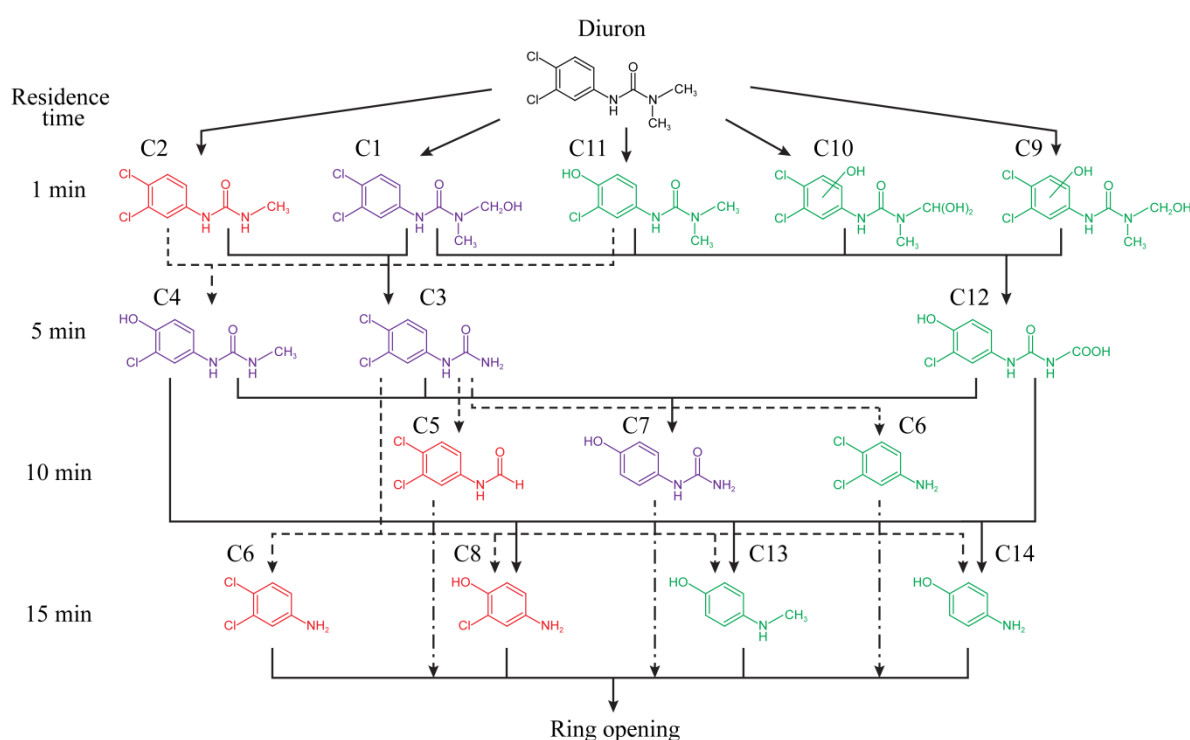


Fig. 6. Structures of diuron degradation intermediates identified by LC-MS/MS and proposed degradation pathway. Intermediates shown in red and green were detected when ZnO nanorods and conventional ZnO particles were used as the catalyst, respectively. Those shown in purple are common intermediates detected using both types of catalyst.

Figures 6 and 7 show that molecular structures of the intermediates, hence the degradation pathways, are affected by type of the catalyst used. Only a few intermediates are commonly formed by the reactions on both catalysts. The difference in the intermediates is noticed even at the shortest residence time investigated, at which the intermediates are assumed to be direct products from the degradation of the parent compounds. On ZnO nanorods, the structures of the generated intermediates (i.e., C1, C2, C15, C16, and C17) suggest that both diuron and linuron are attacked by hydroxyl radicals only on the aliphatic chain of the molecules. There is no sign of an attack on the aromatic side within short residence time. On the other hand, all intermediates formed by the attack of the hydroxyl radicals on the aromatic ring (i.e., C9, C10, C11, C18, C19, and C20) occur only when the conventional ZnO particles are used. In fact, C9, C10, and C19 are formed by simultaneous attacks on both aliphatic and aromatic parts of the molecule.

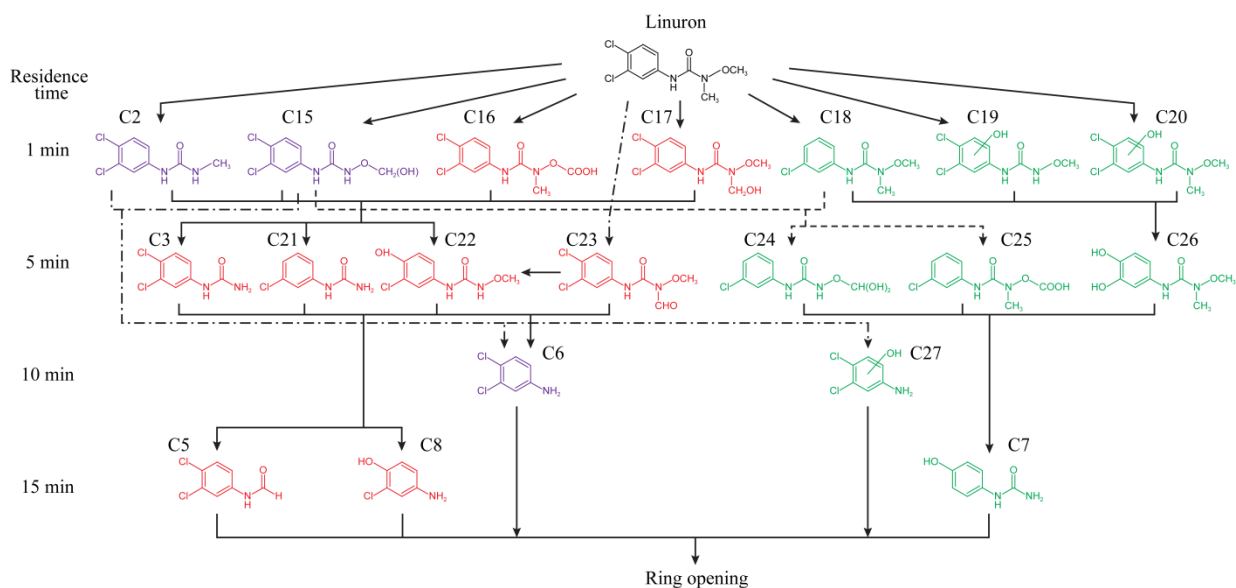


Fig. 7. Structures of linuron degradation intermediates identified by LC-MS/MS and proposed degradation pathway. Intermediates shown in red and green were detected when ZnO nanorods and conventional ZnO particles were used as the catalyst, respectively. Those shown in purple are common intermediates detected using both types of catalyst.

The structures of the intermediates directly derived from diuron and linuron are consistent with the discussion on the adsorption of diuron and linuron on different surfaces of ZnO. Electrons are localized in many parts throughout the molecules of diuron and linuron, e.g., oxygen atom of the carbonyl group, nitrogen atom of the amine group, and chlorine atoms on the aromatic ring, making them negatively charged. Electron withdrawal toward these high-electronegativity atoms results in positive charges on the adjacent atoms. Adjustment of the molecules to turn its negatively charged parts toward the zinc-terminated surface of the conventional ZnO particles, which is uniformly positively-charged, enables the adsorption configuration to be planar; hence allow the attack of the hydroxyl radicals to take place on both sides of the molecules. Similar configuration should also be possible for the adsorption on oxygen-terminated surface. On the other hand, the mixed-terminated surface of the ZnO nanorods is consisted of alternating zinc and oxygen atoms, which is unlikely to match charge distribution on the molecule of either diuron or linuron. Therefore, only the aliphatic side of the molecules, which contains the highest charged functional group, should adsorb onto the mixed-terminated surface and should be mainly attacked by the hydroxyl radicals.

By nature of physical adsorption, the intermediates formed can easily desorb from the surface. As the residence time is prolonged, the intermediates re-adsorb and undergo further degradation until mineralization is achieved. The structures of the subsequent intermediates should therefore depend on the adsorption characteristics of the products from the prior step in the pathway.

4. Conclusion

Residual phenyl urea herbicides in water could be successfully degraded by photocatalytic degradation on zinc oxide. However, the degradations on different surfaces are markedly different, both in rate of the reaction on the surface and the degradation pathway, i.e., the structures of the intermediates formed. Adsorption configuration on the surface of the catalyst, which is surface dependent, is a crucial factor affecting the degradation. The degradation takes place on both aliphatic and aromatic sides of diuron and linuron when the ZnO catalyst is consisted mainly by polar surfaces. On the other hand, on the non-polar mixed-terminated surface, only the aliphatic side is attacked by hydroxyl radicals. Hence, the structure of the catalyst is a crucial factor in determining the dominant degradation pathway.

Acknowledgments

This research was funded by the Ratchadapisek Sompoch Endowment Fund (2016), Chulalongkorn University (CU-59-024-FW).

References

- [1] J. M. Dabrowski, J. M. Shadung, and V. Wepener, "Prioritizing agricultural pesticides used in South Africa based on their environmental mobility and potential human health effects," *Environ. Int.*, vol. 62, pp. 31-40, 2014.
- [2] L. W. Hall, Jr. and R. D. Anderson, "Temporal trends analysis of 2004 to 2012 toxicity and pesticide data for California's Central Valley water quality coalitions," *J. Environ. Sci. Heal. A*, vol. 49, pp. 313-326, 2014.
- [3] S. Hasenbein, S. P. Lawler, and R. E. Connon, "An assessment of direct and indirect effects of two herbicides on aquatic communities," *Environ. Toxicol. Chem.*, vol. 36, pp. 2234-2244, 2017.
- [4] C. Bouquet-Somrani, F. Fajula, A. Finiels, P. Graffin, P. Geneste, and J.-L. Olive, "Photocatalytic degradative oxidation of diuron in organic and semi-aqueous systems over titanium dioxide catalyst," *New J. Chem.*, vol. 24, pp. 999-1002, 2000.
- [5] T. Céline, B. Philippe, S. Martine, B. Frédérique, T. Landoald, C. Annie, B. Jacques, and V. Henri, "Fungal biodegradation of a phenylurea herbicide, diuron: Structure and toxicity of metabolites," *Pest. Manag. Sci.*, vol. 56, pp. 455-462, 2000.
- [6] K. Sun, Z. Zhang, B. Gao, Z. Wang, D. Xu, J. Jin, and X. Liu, "Adsorption of diuron, fluridone and norflurazon on single-walled and multi-walled carbon nanotubes," *Sci. Total. Environ.*, vol. 439, pp. 1-7, 2012.
- [7] N. Boonprakob, W. Chomkitichai, J. Ketwaraporn, A. Wanaek, B. Inceesungvorn, and S. Phanichphant, "Photocatalytic degradation of phenol over highly visible-light active BiOI/TiO₂ nanocomposite photocatalyst," *Engineering Journal*, vol. 21, no. 1, pp. 81-91, 2017.
- [8] G. Pansamut, T. Charinpanitkul, and A. Suriyawong, "Removal of humic acid by photocatalytic process: Effect of light intensity," *Engineering Journal*, vol. 17, no. 3, pp. 25-32, 2013.
- [9] D. Lawless, N. Serpone, and D. Meisel, "Role of hydroxyl radicals and trapped holes in photocatalysis. A pulse radiolysis study," *J. Phys. Chem.*, vol. 95, pp. 5166-5170, 1991.
- [10] M. Carrier, C. Guillard, M. Besson, C. Bordes, and H. Chermette, "Photocatalytic degradation of diuron: Experimental analyses and simulation of HO^o radical attacks by density functional theory calculations," *J. Phys. Chem. A*, vol. 113, pp. 6365-6374, 2009.
- [11] K. Hana, K. Josef, M. Kateřina, and J. Jaromír, "Photocatalytic degradation of diuron [3-(3,4-dichlorophenyl)-1,1-dimethylurea] on the layer of TiO₂ particles in the batch mode plate film reactor," *J. Chem. Technol. Biot.*, vol. 72, pp. 169-175, 1998.
- [12] S. Malato, J. Cáceres, A. R. Fernández-Alba, L. Piedra, M. D. Hernando, A. Agüera, and J. Vial, "Photocatalytic treatment of diuron by solar photocatalysis: Evaluation of main intermediates and toxicity," *Environ. Sci. Technol.*, vol. 37, pp. 2516-2524, 2003.
- [13] E. Evgenidou, I. Konstantinou, K. Fytianos, and T. Albanis, "Study of the removal of dichlorvos and dimethoate in a titanium dioxide mediated photocatalytic process through the examination of intermediates and the reaction mechanism," *J. Hazard. Mater.*, vol. 137, pp. 1056-1064, 2006.
- [14] O. T. Woo, W. K. Chung, K. H. Wong, A. T. Chow, and P. K. Wong, "Photocatalytic oxidation of polycyclic aromatic hydrocarbons: Intermediates identification and toxicity testing," *J. Hazard. Mater.*, vol. 168, pp. 1192-1199, 2009.
- [15] V. Kruefu, H. Ninsonti, N. Wetchakun, B. Inceesungvorn, P. Pookmanee, and S. Phanichphant, "Photocatalytic degradation of phenol using Nb-loaded ZnO nanoparticles," *Engineering Journal*, vol. 16, no. 3, pp. 91-99, 2012.
- [16] W. Khongthon, G. Jovanovic, A. Yokochi, P. Sangvanich, and V. Pavarajarn, "Degradation of diuron via an electrochemical advanced oxidation process in a microscale-based reactor," *Chem. Eng. J.*, vol. 292, pp. 298-307, 2016.
- [17] B. H. Hameed, A. L. Ahmad, and K. N. A. Latiff, "Adsorption of basic dye (methylene blue) onto activated carbon prepared from rattan sawdust," *Dyes Pigments*, vol. 75, pp. 143-149, 2007.

- [18] A. Kornherr, S. A. French, A. A. Sokol, C. R. A. Catlow, S. Hansal, W. E. G. Hansal, J. O. Besenhard, H. Kronberger, G. E. Nauer, and G. Zifferer, "Interaction of adsorbed organosilanes with polar zinc oxide surfaces: A molecular dynamics study comparing two models for the metal oxide surface," *Chem. Phys. Lett.*, vol. 393, pp. 107-111, 2004.
- [19] A. Kornherr, G. E. Nauer, A. A. Sokol, S. A. French, C. R. A. Catlow, and G. Zifferer, "Adsorption of organosilanes at a Zn-Terminated ZnO (0001) surface: Molecular dynamics study," *Langmuir*, vol. 22, pp. 8036-8042, 2006.
- [20] M. Ebato and K. Yonebayashi, "Method for estimating competitive adsorption of herbicides on soils," *J. Pestic. Sci.*, vol. 30, pp. 220-224, 2005.
- [21] F. Zhang, B. Liu, G. Liu, Y. Zhang, J. Wang, and S. Wang, "Substructure-activity relationship studies on antibody recognition for phenylurea compounds using competitive immunoassay and computational chemistry," *Sci. Rep.*, vol. 8, pp. 3131, 2018.
- [22] T. Steiner, "The hydrogen bond in the solid state," *Angew. Chem. Int. Edit.*, vol. 41, pp. 48-76, 2002.
- [23] V. Sasikala, D. Sajan, L. Joseph, B. Narayana, and B. K. Sarojini, "Spectroscopic and non-linear optical studies of two novel optical limiters from dichloroaniline family crystals: 3,4-Dichloroaniline and 3,5-dichloroaniline," *Opt. Laser Technol.*, vol. 96, pp. 23-42, 2017.
- [24] J. F. Montoya, M. F. Atitar, D. W. Bahnemann, J. Peral, and P. Salvador, "Comprehensive kinetic and mechanistic analysis of TiO₂ photocatalytic reactions according to the direct-indirect model: (II) Experimental validation," *J. Phys. Chem. C*, vol. 118, pp. 14276-14290, 2014.
- [25] S. Chusaksri, J. Lomda, T. Saleepochn, and P. Sutthivaiyakit, "Photocatalytic degradation of 3,4-dichlorophenylurea in aqueous gold nanoparticles-modified titanium dioxide suspension under simulated solar light," *J. Hazard. Mater.*, vol. 190, pp. 930-937, 2011.
- [26] M. J. Farré, S. Brosillon, X. Domènech, and J. Peral, "Evaluation of the intermediates generated during the degradation of diuron and linuron herbicides by the photo-Fenton reaction," *J. Photoch. Photobiol. A*, vol. 189, pp. 364-373, 2007.
- [27] H. Katsumata, M. Sada, Y. Nakaoka, S. Kaneco, T. Suzuki, and K. Ohta, "Photocatalytic degradation of diuron in aqueous solution by platinized TiO₂," *J. Hazard. Mater.*, vol. 171, pp. 1081-1087, 2009.
- [28] S. Meephon, T. Rungrotmongkol, N. Kaiyawet, S. Puttamat, and V. Pavarajarn, "Surface-dependence of adsorption and its influence on heterogeneous photocatalytic reaction: A case of photocatalytic degradation of linuron on zinc oxide," *Catal. Lett.*, vol. 148, pp. 873-881, 2018.
- [29] L. H. Mendoza-Huizar, "Chemical reactivity of isoproturon, diuron, linuron, and chlorotoluron herbicides in aqueous phase: A theoretical quantum study employing global and local reactivity descriptors," *J. Chem.*, vol. 2015, p. 9, 2015.
- [30] R. G. Pearson, "Chemical hardness and bond dissociation energies," *J. Am. Chem. Soc.*, vol. 110, pp. 7684-7690, 1988.